Synthesis and thermal decomposition study of dysprosium trifluoroacetate

Opata, Y. A.; Grivel, J.-C.

Published in:
Journal of Analytical and Applied Pyrolysis

Link to article, DOI:
10.1016/j.jaap.2018.03.018

Publication date:
2018

Document Version
Peer reviewed version

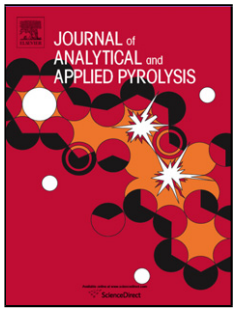

Title: Synthesis and Thermal decomposition study of Dysprosium Trifluoroacetate

Authors: Y.A. Opata, J.-C. Grivel

PII: S0165-2370(17)30907-5
DOI: https://doi.org/10.1016/j.jaap.2018.03.018
Reference: JAAP 4292

To appear in: *J. Anal. Appl. Pyrolysis*

Received date: 11-10-2017
Revised date: 13-3-2018
Accepted date: 18-3-2018

Please cite this article as: Y.A.Opata, J.-C.Grivel, Synthesis and Thermal decomposition study of Dysprosium Trifluoroacetate, Journal of Analytical and Applied Pyrolysis https://doi.org/10.1016/j.jaap.2018.03.018

Synthesis and Thermal decomposition study of Dysprosium Trifluoroacetate

Y. A. Opata* and J-C. Grivel

Department of Energy Conversion and Storage, Technical university of Denmark

Frederiksborgvej 399, 4000 Roskilde, Denmark

***Corresponding author:** Tel.: +45 46775899

E-mail address: yaop@dtu.dk, yuriopata@gmail.com (Yuri A. Opata)

Highlights

- The thermal decomposition process of the dysprosium trifluoroacetate has been investigated.
- The presence of some carbon is verified in the system after decomposition stage.
- Formation of the DyF_3 and DyOF phases are confirmed by TG and x-ray diffraction data.
- Analysis of the gases released following the entire decomposition process.

Abstract

A study of the thermal decomposition process of dysprosium trifluoroacetate hydrate under flowing argon is presented. Thermogravimetry, differential thermal analysis, evolved gas analysis and ex-situ x-ray diffraction techniques have been employed in the investigation. Three main stages were identified: dehydration, decomposition and phase transformation from DyF_3 to DyFO. The dehydration takes place in 2 steps and the decomposition also occurs in two stages. The observed residual mass demonstrated a discrepancy with the calculated value for DyF_3 formation. Observations on quenched samples at temperatures just above the decomposition step and at 828°C showed a variation in the sample color, being dark in the first case and rather bright at the higher quenching temperature. Based on this fact, we concluded that some carbon remains in the

sample up to 800°C. With the temperature reaching 1300°C, a plateau is observed in the TG signal, which mass value agrees with the formation of DyFO as verified by the ex-situ x-ray data of quenched powder. Using the FTIR and MS spectra of released gases during the process and the TG data, a decomposition scheme is suggested.

Keywords: Thermal decomposition, dysprosium trifluoroacetate, TG, DTA, FTIR and mass spectrometry.

1. Introduction

Trifluoroacetate (TFA) precursors are being widely used for the manufacture of high performance high-temperature superconducting (HTS) coated conductors and thin film, processed through the chemical solution decomposition (CSD) method [1]-[7]. The manufacture of HTS coated conductors beneficiates from a prior knowledge of the (metal) TFA thermal decomposition mechanism, by allowing the determination and optimization of the involved pyrolysis and reaction processes. Therefore, an increasing number of studies on the thermal decomposition of TFA complexes have been made in the past years [8]-[10]. Earlier, Rillings had investigated the thermal decomposition of the Pr, Sm and Er trifluoroacetate compounds in air and vacuum, wherever the formation of LnF_3 and LnOF (Ln=Pr,Sm and Er) was ascertained [11]. IR measurements of the volatile products revealed the presence of CO, CO_2, CF_3COF and $(CF_3CO)_2O$. Based on these results the following decomposition scheme was proposed: $Ln(CF_3COO)_3$ -> LnF_3 + $(CF_3CO)_2$ + CO_2 + CO. A similar study carried out under static air, covering all lanthanide trifluoroacetate complexes, was reported in [12]. Through TG and DTA experiments the LnF_3 formation as final solid residue (now with Ln=La-Lu, except Pm), at temperatures between 300°C and 550°C, was also confirmed.

The thermal behavior of Dy(TFA), which is used as a precursor in the preparation of $DyBa_2Cu_3O_{7-\delta}$ superconducting thin films and coated conductors [1] still deserves additional studies. In particular, the exact nature of the gas species released during the decomposition process is not clear, because the use of static air, as used in [12], results in combustion of organic materials. This kind of strongly exothermic reaction induces local overheating in the sample that can potentially disturb the reaction course mechanism and, in particular, its kinetics. Furthermore, the manufacture of rare-earth cuprate HTS coated conductors imposes the use of low

oxygen partial pressure [13], thus, thermal decomposition studies in Ar are important to complete previous work made in air as well as an excellent starting point for more specific investigations with precisely controlled low pO_2 conditions. With this in view, the present work reports on a thermal decomposition study of $Dy(CF_3COO)_3$ under flowing argon gas, based on simultaneous TG-DTA, while the nature of the gases released during the process were investigated using FTIR and MS spectroscopic methods and phase changes were followed by means of in-situ high temperature x-ray measurements.

2. Material and methods

Dysprosium trifluoroacetate, $Dy(CF_3COO)_3$, was synthesized from dysprosium acetate tetrahydrate, $Dy(CH_3COO)_3 \cdot 4H_2O$, supplied by Alfa Aesar 99.9% purity-metal basis (MB), following a procedure similar to that applied for the preparation of $DyBa_2Cu_3O_{7-\delta}$ precursor solutions [1]. The same MB purity is expected for the synthesized $Dy(CF_3COO)_3$, since no other metallic cations have been involved in the process. Approximately 2 g of $Dy(CH_3COO)_3 \cdot 4H_2O$ were mixed with 3.5 ml trifluoroacetic acid (99.9% from Alfa Aesar) and 10 ml deionized water. The solution was being stirred on a hot plate during 2 hours at 50°C and, after reaction, was heated at about 100°C to evaporate the excess solvent. TG and DTA measurements were carried out in a NETZSCH model STA 449C simultaneous TG-DTA, using Ar gas flow (with 0.5 ppm residual O_2 content). Sample masses of 20 mg were used for this purpose. The powder was loaded into uncovered alumina crucibles. The samples were heated from room temperature to 1450°C at 2 K/min with a gas flow of 50 ml/min. The signals were afterwards corrected by subtracting a base line curve, obtained on an empty crucible with the same heating profile. FTIR spectra of the evolved gases resulting from decomposition were recorded simultaneously with the TG-DTA measurements using a BRUKER, model TENSOR27 spectrometer connected to the TG-DTA equipment by a hot line maintained at 200°C. Mass spectrometry was also used to identify the released gases, employing a NETZSCH – QMS 403 D Aëolos mass spectrometer linked by a quartz glass capillary, heated to 200°C, to a NETZSCH - STA 409CD thermobalance. The mass spectra were collected and analyzed in the 1-299 m/z range. The conditions of sample mass, temperature, heating rate and gas flow for the MS experiments were the same used in the TG-DTA. Ex-situ x-ray measurements, carried out on quenched samples, were

employed to investigate the crystallographic phase. A Rigaku diffractometer was used to collect the x-ray patterns from 2θ = 25° to 70° with a scan speed of 1°/min.

3. Results and discussion

The XRD pattern and FTIR spectrum of the as-prepared sample powder are displayed in Figure 1(a) and (b), respectively. The XRD data show that the compound is well crystallized and confirm that the sample consists of the $Dy(CF_3COO)_3 \bullet 3H_2O$ phase, by comparison with the reference data (JCPD files number 052-0724). Furthermore, the absorption bands observed in the FTIR spectrum match those reported in [14]-[16] for RE-TFA salts, RE = Y, Sm, Eu, Er and Yb, which are expected to exhibit similar absorption bands.

Figure 2 shows the thermal analysis results obtained under 50 ml/min argon gas flow. The first two steps in the TG curve (peaks at 86°C and 125°C in the DTG and DTA traces) are associated to the loss of water, as confirmed by the solid residue and evolved gas FTIR measurements, showed in Figure 3 and 5(b) respectively. In the latter, broad peaks in the 3750-3000 cm^{-1} region, assigned to νOH vibrations [15], are observed in the as-prepared powder, whereas the FTIR spectrum obtained from the powder quenched at 200°C does not present similar peaks, evidencing the complete release of water. From the TG trace the amount of disassociated water during these first stages can be estimated as 1.62 ± 0.02 and 1.10 ± 0.05 water molecules. A dehydration process taking place in two or more steps was also found for other RE(TFA) compounds, with quantities of dissociated water being observed between 1 and 3.7 molecules of H_2O per formula unit [8, 12, 17]. Upon further heating, a small endothermic peak (at 239°C) is observed, accompanied by some mass change. A similar peak was reported in [11] and [12], where it was assigned to a “solution effect” involving the anhydrous precursor dissolved in some water of hydration. A similar behavior of the DTA and TG traces was also reported in [18], but in that case it was assumed to be due to a partial decarboxylation of the anhydrous compound. According to the mass spectra data (see Figure 6), carbon dioxide fragments, among other precursors, are detected at around 233°C, indicating that the endothermic peak might be related to a decarboxylation process. At 280°C the $Dy(CF_3COO)_3$ anhydrous phase exhibits a large mass loss, related to its decomposition, achieving a plateau with

a mass of 41.9% of the initial sample mass, at around 350°C. Based on previous studies on trifluoroacetate compounds [8, 11, 12, 17], DyF_3 would be expected to form after the decomposition of the TFA ligands. However the observed sample mass is still higher than the one calculated for the formation of DyF_3 (39.8%) - see dashed horizontal lines in Figure 2. A possible reason is that some carbon remains in the sample (about 0.9 carbon atoms per DyF_3 molecule on average would account for the observed sample mass). By quenching the sample at 405°C, one can observe a dark coloring (see inset picture in Figure 2), whereas a sample quenched at 828°C – the temperature at which the observed sample mass matches with that calculated for DyF_3 - a lighter color is observed. This supports the assumption that elemental carbon was left in the sample at 405°C, before being oxidized and released in the form of CO_2 or CO at higher temperature. Finally, close to the maximum temperature, the TG curve reaches a plateau, with mass of 35.3%. Such value agrees with the formation of DyFO (35.8%).

FTIR results, acquired from samples quenched at different temperatures, are presented in Figure 3. The spectrum of the as-grown sample from Figure 1(b) is displayed again for comparison purpose. The heating rate employed was the same as that used for the TG measurements. A strong well-defined triplet absorption band in the region 1723-1619 cm^{-1}, associated to CO_2 vibrations, suggests chelating-bridging TFA for the as-prepared sample [15]. On the other hand, the spectrum acquired at 200°C shows a single broad peak at 1640 cm^{-1} in the same range, which might be due a different bonding of the trifluoroacetate ligands [15, 16]. Another characteristic peak from TFA [9, 14, 15, 19] is also observed in the region 1473-1487 and is related to νsCO_2. A doublet at 1204-1143 due to νC-F and νC-O vibrations and bands in the 855-609 cm^{-1} region, supposedly from $\delta sFCF_2$, $\delta asCF_3$ and $\delta asFCF_2$ [15, 19] are also observable. The complete TFA ligands decomposition is verified in the spectrum recorded at 405°C, where no characteristic peaks are observed.

Figure 4 displays the x-ray patterns recorded from solid residue obtained after quenching the samples from the indicated temperatures. The heating rate and gas conditions employed here were the same as in the TG experiments. Using the powder diffraction file PDF2 database, the following phases were identified: orthorhombic DyF_3 (JCPD files number 032-0352) and rhombohedral DyFO (JCPD files number 019-0437), for the powder quenched at 405°C and 1280°C, respectively. The apparent peaks observed in the XRD pattern from

sample quenched at 1280°C on both sides of the DyOF reflection at 2θ = 28.6° are artefacts resulting from the subtraction of the sample-holder and the low intensity signal from the powder sample. For the sample treated up to 826°C we note the presence of DyF_3 with some reflections from rhombohedral and cubic DyFO (JCPD files number 033-0524). These results are in good agreement with the mass evolution data observed from the TG curve, where DyF_3 is expected to be found up to 830°C and DyFO at higher temperatures.

Figure 5(a) presents the FTIR evolved gas analysis spectra, acquired during the Dy(TFA) heating, around the main mass loss in Figure 2. Gas species are first detected at 256°C, with the observation of small amounts of CO_2 (2353 and 2328 cm^{-1}) and CO (2176 and 2115 cm^{-1}) and absorption bands at 1829, 1784, 1213 and 1120 cm^{-1} from CF_3COF, $(CF_3CO)_2O$ and CF_3COOH. With the increase in temperature, COF_2, CF_3COF, $(CF_3CO)_2O$ emissions are also identified, as well as a minor peak at 1155 cm^{-1} from CHF_3. All the identified absorption bands are summarized in Table 1. Similar characteristic absorption bands were also observed during the thermal decomposition of $Y(CF_3COO)_3$ [17] and $Cu(CF_3COO)_2$ [10]. Figure 5(b) shows the collected FTIR spectra of detected gases around 89°C and 131°C, which further confirm the release of water [20] observed in the Figure 2 at similar temperatures.

From mass spectroscopy experiments (Figure 6) it was possible to confirm the interpretation of the FTIR data. One can notice on Figure 6(a) that the main fragments are related to $[CO_2]^+$ (m/z=44), which follows the DTG curve rather well, and $[F]^+$ (m/z=19). CF_3COOH, COF_2, $(CF_3CO)_2O$ and CF_3CFO species were evidenced by $[COOH]^+$ (m/z= 45), (m/z=66) $[COF_2]^+$, (m/z=97) $[CF_3CO]^+$ and (m/z=47) $[COF]^+$ observation, respectively, whereas peaks (m/z=31) $[CF]^+$, (m/z=50) $[CF_2]^+$ and (m/z=69) $[CF_3]^+$ might result from the contribution of all of them.

The peaks m/z=12, 16 and 22 are also from CO_2 fragmentation and present an evolution similar to that of m/z=44. Two other peaks that were detected with non-negligible intensity are m/z = 15 and 43, which could be ascribed to fragments of CH_3COO and CH_3COCH_3 [21, 22]. These might originate from the decomposition of remnants unreacted starting material $Dy(CH3COO)_3$. Minor intensities from $[CF_2]^{++}$ (m/z=25) and $[CF_3CFO]^+$ (m/z=116) are also observed around the main peak of Figure 2, the latter being associated to the CF_3COF compound. A look at Figure 6(b) reveals the presence of the $[CHF_2]^+$ (m/z=51) ion, which can be due to either

CF_3COOH or CHF_3. At around 270°C its evolution is similar to that of m/z=45, however it presents a secondary peak at 315°C, not observed for $[COF]^+$. The FTIR results indicate the formation of CHF_3 at elevated temperature (~290°C), which suggests that this peak is a contribution from both CF_3COOH and CHF_3 compounds. The data in Figure 6 reveals furthermore that the decomposition process occurs in two stages, as also reported for other trifluoroacetate compounds [9, 23]. At around 233°C, peaks in the signals m/z = 12, 16, 17, 18, 22, 44 and 45 are observed. These fragments are associated to the release of CO_2, H_2O and CF_3COOH, as already mentioned. Therefore, the endothermic peak observed in the DTA signal (Figure 2) at around 239°C might actually be attributed to a decarboxylation process rather than to a boiling effect. In addition, the detected CF_3COOH appears as a result of the reaction between $(CF_3CO)_2O$ and water as describe below in the text.

Based on the presented results, the following set of reactions is proposed. First, as indicated by equations (1-1), (1-2) and (2), dehydration of the Dy(TFA) takes place, as clearly observed in the inset of Figure 6, where the $[H_2O]^+$ (m/z=18) and $[OH]^+$ (m/z=17) ion emissions were observed. Then TFA decomposition takes place, resulting in the DyF_3+C, $(CF_3CO)_2O$, CO and O_2 formation. Herein, carbon remains in the sample after $Dy(CF_3COO)_3$ decomposition, as suggested by the TG results as well as by the dark color of the powder. In the case where all TFA ligands have been removed, the expected reaction [8, 11, 12, 17] would be as indicated by equation (3).

$$Dy(CF_3COO)_3 \bullet 2.7H_2O \rightarrow Dy(CF_3COO)_3 \bullet 1.6H_2O + 1.1H_2O \quad (1\text{-}1)$$

$$Dy(CF_3COO)_3 \bullet 1.6H_2O \rightarrow Dy(CF_3COO)_3 + 1.6H_2O \quad (1\text{-}2)$$

$$Dy(CF_3COO)_3 \rightarrow DyF_3 + C + (CF_3CO)_2O + CO + O_2 \quad (2)$$

$$Dy(CF_3COO)_3 \rightarrow DyF_3 + (CF_3CO)_2O + CO + CO_2 \quad (3)$$

As some CF_3COOH was detected both by FTIR and MS, it is suggested that some water vapor was trapped in the sample and reacted with $(CF_3CO)_2O$, forming trifluoroacetic acid following [8, 17], according to reaction (4). This CF_3COOH later decomposes into CF_2, HF and CO_2 [10, 17], as suggested by the $[CF_2]^{++}$ (m/z=25) and $[CF_2]^+$ (m/z=50), $[F]^+$ (m/z=19) and $[CO_2]^+$ (m/z=44) detection in the MS data.

$$(CF_3CO)_2O + H_2O \rightarrow 2CF_3COOH \quad (4)$$

$$CF_3COOH \rightarrow CF_2 + HF + CO_2 \quad (5)$$

$$CF_2 + HF \rightarrow CHF_3 \quad (6)$$

As already mentioned above, the observation of CHF_3 by FTIR and MS could be the result of a side reaction between CF_2 and HF, resulting in a minor detection [9, 17]. Finally, once all the available water has been used for the CF_3COOH forming reaction, it is probable that $(CF_3CO)_2O$ decomposes as indicated in [8, 11, 12, 17], according to:

$$(CF_3CO)_2O \rightarrow CF_3COF + COF_2 + CO \quad (7)$$

4. **Conclusions**

The thermal decomposition of dysprosium trifluoroacetate hydrate, as well as the evolved gas species released during the process, was investigated by means of TG-DTA, FTIR/MS and ex-situ x-ray diffraction. Two mass-loss steps were observed in the first stage of heating up to 195°C, and could be assigned to two dehydration processes, wherein the loss of around 2.7 water molecules take place. Further heating results in a small endothermic peak at 239°C, an event that can be ascribed, based on the mass spectroscopy results, to a decarboxylation process. The decomposition process is then characterized by an intense exothermic peak centered at 280°C, accompanied by a 49% mass reduction of the sample. FTIR and MS spectra analyzes of released volatile compounds enable the identification of CF_3COF, $(CF_3CO)_2O$, CHF_3, CF_3COOH, COF_2, CO_2 and CO. Previous investigations about the decomposition process of M(TFA) precursors (M = lanthanide elements) have demonstrated the formation of MF_3 phases after the decomposition process [11, 12]. However, in our case, the resulting residual sample mass after decomposition showed a value higher (42.0%) than the calculated one (39.8%). Pictures of quenched samples, heated under similar conditions as in the TG experiments, revealed a dark coloration of the sample quenched at 405°C (end of the decomposition process) and a brighter color in that heated up to 828°C. Therefore, we believe that some carbon remained in the sample. At 1300°C, the

sample mass reached a plateau, with a value corresponding to the formation of DyFO formation. Analyzes of x-ray diffraction patterns, collected from quenched samples, revealed the formation of DyF_3 up to 830°C and DyFO phase for elevate temperatures. Based on all obtained results, a decomposition scheme was established. Further work is in progress to study and understand the influence of oxidating and/or water saturated atmospheres on the thermal decomposition of this compound, conditions that will be closer to those used for the manufacture of RE123 superconducting thin films.

Acknowledgements

This work was supported by the Brazilian program Science without borders – Proc. Number BEX 13491/13-0.

References

[1] Y. A. Opata, A. C. Wulff, J. O. B. Hansen, Y. Zhao and J-C. Grivel. Superconducting $Dy_{1-x}(Gd,Yb)_xBa_2Cu_3O_{7-\delta}$ thin films made by Chemical Solution Deposition. IEEE Transactions on Applied Superconductivity, 26(3) (2016) 7500705 (5pp).

[2] Y. Zhao, W. Wu, X. Tang, N. H. Andersen, Z. Han and J-C. Grivel. Epitaxial growth of $YBa_2Cu_3O_{7-x}$ films on $Ce_{0.9}La_{0.1}O_{2-y}$ buffered yttria-stabilized zirconia substrates by an all-chemical-solution route. CrystEngComm, 16 (2014) 4369-4372.

[3] K. De Keukeleere, P. Cayado, A. Meledin, F. Vallès, J. De Roo, H. Rijckaert, G. Pollefeyt, E. Bruneel, A. Palau, M. Coll, S. Ricart, G. Van Tendeloo, T. Puig, X. Obradors and I. Van Driessche. Superconducting $YBa_2Cu_3O_{7-\delta}$ Nanocomposites Using Preformed ZrO_2 Nanocrystals: Growth Mechanisms and Vortex Pinning Properties. Advanced Electronic Materials, 2 (2016) 1600161 (9pp).

[4] P. Abellán , F. Sandiumenge, M-J. Casanove, M. Gibert, A. Palau, T. Puig and X. Obradors. Interaction between solution derived $BaZrO_3$ nanodot interfacial templates and $YBa_2Cu_3O_7$ films leading to enhanced critical currents. Acta Materialia 59 (2011) 2075–2082.

[5] Y. Xu, H-L. Suo, Y. Zhao, J-C. Grivel and M. Liu. Jc Enhancement by La-Al-O Doping in Y-Ba-Cu-O Films Both in Self-Field and Under Magnetic Field. IEEE Transactions on Applied Superconductivity, 26(3) (2016) 6602804 (4pp).

[6] T. Qureishy, Y. Zhao, Y. Xu, J. I. Vestgården, T. H. Johansen, J-C. Grivel, H. Suo, P. Mikheenko. Magnetic flux channelling in YBa2Cu3O7-δ films grown by a chemical solution deposition technique on vicinal and non-vicinal substrates. Advanced Materials Letters, 8 (2017) 1204-1210.

[7] P. Garcés, M. Coll, H. Castro, T. Puig and X. Obradors. Preparation of YBCO-BYTO and YBCO-BZO nanostructured superconducting films by chemical method. Journal of Physics. Conference Series, 786 (2017) 012017 (5pp).

[8] H. Eloussifi, J. Farjas, P. Roura, J. Camps, M. Dammak, S. Ricart, T. Puig and X. Obradors. Evolution of yttrium trifluoroacetate during thermal decomposition. Journal of Thermal Analysis and Calorimetry, 108 (2012) 589–596.

[9] J. Farjas, J. Camps, P. Roura, S. Ricart, T. Puig and X. Obradors. The thermal decomposition of barium trifluoroacetate. Thermochimica Acta, 544 (2012) 77-83.

[10] M. Mosiadz, K. L. Juda, S. C. Hopkins, J. Soloducho and B. A. Glowacki. An in-depth in situ IR study of the thermal decomposition of copper trifluoroacetate hydrate. Journal of Fluorine Chemistry, 135 (2012) 59-67.

[11] K. W. Rillings and J. E. Roberts. A thermal study of the trifluoroacetates and pentafluoropropionates of praseodymium, samarium and erbium. Thermochimica Acta, 10 (1974) 285-298.

[12] Y. Yoshimura and K. Ohara. Thermochemical studies on the lanthanoid complexes of trifluoroacetic acid. Journal of alloys and compounds, 408-412 (2006) 573-576.

[13] R. Feenstra, T. B. Lindemer, J. D. Budai and M. D. Galloway. Effect of pressure on the synthesis of $YBa_2Cu_3O_{7-X}$ thin films by post-deposited annealing. Journal of Applied Physics, 69 (1991) 6569-6585.

[14] V. Y. Kavun, T. A. Kaidalova, V. I. Kostin, E. S. Panin and B. N. Chernyshov. X-ray-diffraction and IR spectroscopic study of crystallohydrates trifluoroacetates of samarium, europium, erbium and ytterbium. Koordinatsionnaya Khimiya, 10 (1984) 1502-1504.

[15] S. Mishra, L. G. Hubert-Pfalzgraf, S. Daniele, M. Rolland, E. Jeanneau and B. Jouguet. Thermal dehydration of $Y(TFA)_3(H_2O)_3$: Synthesis and molecular structures of $[Y(\mu,\eta^1{:}\eta^1\text{-}TFA)_3(THF)(H_2O)_{1\infty}]\bullet THF$ and $[Y_4(\mu_3\text{-}OH)_4(\mu,\eta^1{:}\eta^1\text{-}TFA)_6(\eta^1\text{-}TFA)(\eta^2\text{-}TFA)(THF)_3(DMSO)(H_2O)]\bullet 6THF$ (TFA = trifluoroacetate). Inorganic Chemistry Communications, 12(2) (2009) 97-100.

[16] J. Zhang, S. Morlens, L. G. Hubert-Pfalzgraf and D. Luneau. Synthesis, Characterization and Molecular Structures of Yttrium Trifluoroacetate Complexes with O- and N-Donors: Complexation vs. Hydrolysis. European Journal of Inorganic Chemistry, (2005) 3928-3935.

[17] M. Mosiadz, K. L. Juda, S. C. Hopkins, J. Soloducho and B. A. Glowacki. An in-depth in situ IR study of the thermal decomposition of yttrium trifluoroacetate hydrate. Journal of Thermal Analysis and Calorimetry, 107 (2012) 681–691.

[18] N. P. Sokolova, L. A. Sheludyakova, V. I. Lisoivan, V. P. Fadeeva and S. V. Larionov. Synthesis and Study of Gadolinium(III), Terbium(III), and Dysprosium(III) Trifluoroacetate Trihydrates. Russian Journal of General Chemistry, 67 (1997) 1327-1330.

[19] C. Rüssel. A pyrolytic route to fluoride glasses. I. Preparation and thermal decomposition of metal trifluoroacetates. Journal of Non-Crystalline Solids, 152 (1993) 161-166.

[20] http://webbook.nist.gov/chemistry/form-ser.html.

[21] J. Farjas, J. Camps, P. Roura, S. Ricart, T. Puig and X. Obradors. Thermoanalytical study of the formation mechanism of yttria from yttrium acetate. Thermochimica Acta, 521 (2011) 84-89.

[22] T. Arii, T. Taguchi, Ak. Kishi, M. Ogawa, Y. Sawada. Thermal decomposition of cerium(III) acetate studied with samplecontrolled thermogravimetric–mass spectrometry (SCTG—MS). J. Eur. Ceram. Soc. 22 (2002) 2283-2289.

[23] P. Roura, J. Farjas, H. Eloussifi, L. Carreras, S. Ricart, T. Puig and X. Obradors. Thermal analysis of metal organic precursors for functional oxide preparation: Thin films versus powders. Thermochimica Acta, 601 (2015) 1-8.

[24] D. M. Jollie and P. G. Harrison. An in situ IR study of the thermal decomposition of trifluoroacetic acid. Journal of the Chemical Society, Perkin Transactions 2, (1997) 1571-1575.

[25] R. E. Kagarise. Infrared Spectrum of Trifluoroacetic Acid Vapor. The Journal of Chemical Physics, 27 (1957) 519-522.

[26] N. Fuson and M-L. Josien. Infrared and Raman Spectroscopy Studies of Light and Heavy Trifluoroacetic Acids. The Journal of Chemical Physics, 20 (1952) 1627-1634.

[27] C. V. Berney. Spectroscopy of CF_3COZ compounds—IV: Vibrational spectrum of trifluoroacetyl fluoride. Spectrochimica Acta Part A: Molecular Spectroscopy, 27 (1971) 663-672.

[28] R. L. Redington. Matrix-isolation spectra of ^{18}O-substituted trifluoroacetic acid monomers and vibrational assignments for related CF_3-containing molecules. Spectrochimica Acta Part A: Molecular Spectroscopy, 31 (1975) 1699-1705.

[29] K. Kim and W. T. King. Integrated infrared intensities and atomic polar tensors in fluoroform. The Journal of Chemical Physics, 73 (1980) 5591-5597.

Figure 1 – (a) XRD pattern of the as-prepared sample powder recorded at room temperature. (b) FTIR spectrum of the same sample.

Figure 2 – Double plotting of TG (left) and DTA (right) obtained from heating the sample up to 1450°C at 2 K/min rate in Ar gas flow. Horizontal dashed lines denote the expected residual mass for the formation of: $Dy(CF_3COO)_3 \bullet 2.7H_2O$ (100%); $Dy(CF_3COO)_3 \bullet 1.1H_2O$ (94.7%); $Dy(CF_3COO)_3$ (91.0%); $DyF_3+0.9C$ (42.0%); DyF_3 (39.8%); and DyFO (35.8%). The inset picture shows the quenched samples at 405°C (left) and 828°C (right).

Figure 3 – FTIR spectra obtained from as-prepared $Dy(FTA)_3$ powder and also from the solid residue resulting from heated and quenched samples at 200°C and 405°C. The employed heating profile was the same as used for the TG experiment.

Figure 4 – XRD diffractograms collected from quenched powder at 405°C, 826°C and 1280°C. The broad intensity background around 27°- 35° and 40°- 47°, observed only for the two lower temperatures spectra, is due the sample holder signal. Data obtained for the sample quenched at 1280°C was multiplied by a factor of 2 for better visualization. The identified crystallographic phases are indicated in the figure. The samples were heated employing the same parameters used for the TG-DTA experiments.

Figure 5 – FTIR spectra of gases released from $Dy(TFA)_3 \bullet 2.7H_2O$ during decomposition. The data were recorded simultaneously with the TG measurement, carried out in dry Ar gas flow. The curves are offset for a better visualization. (a) spectra recorded from the temperature region around the decomposition process. Dashed lines point out the center of the band positions, indicated by the respective wavenumber in cm^{-1}. (b) evolved gas spectra detected at around 89°C and 131°C, where only absorption bands from water are observed [20].

Figure 6 – (a) and (b) mass spectrometer data from simultaneous TG-MS experiment. The dashed line indicates the DTG trace (with negative value upwards), while solid lines show the detected ions from Dy(TFA) decomposition. The results refer to the main mass loss region of the TG experiment. The inset in frame (a)

shows the TG (solid line) and DTG (dashed line) curves as well the mass detection related to H_2O (m/z=17 and 18) and F (m/z=19).

Figure 1.

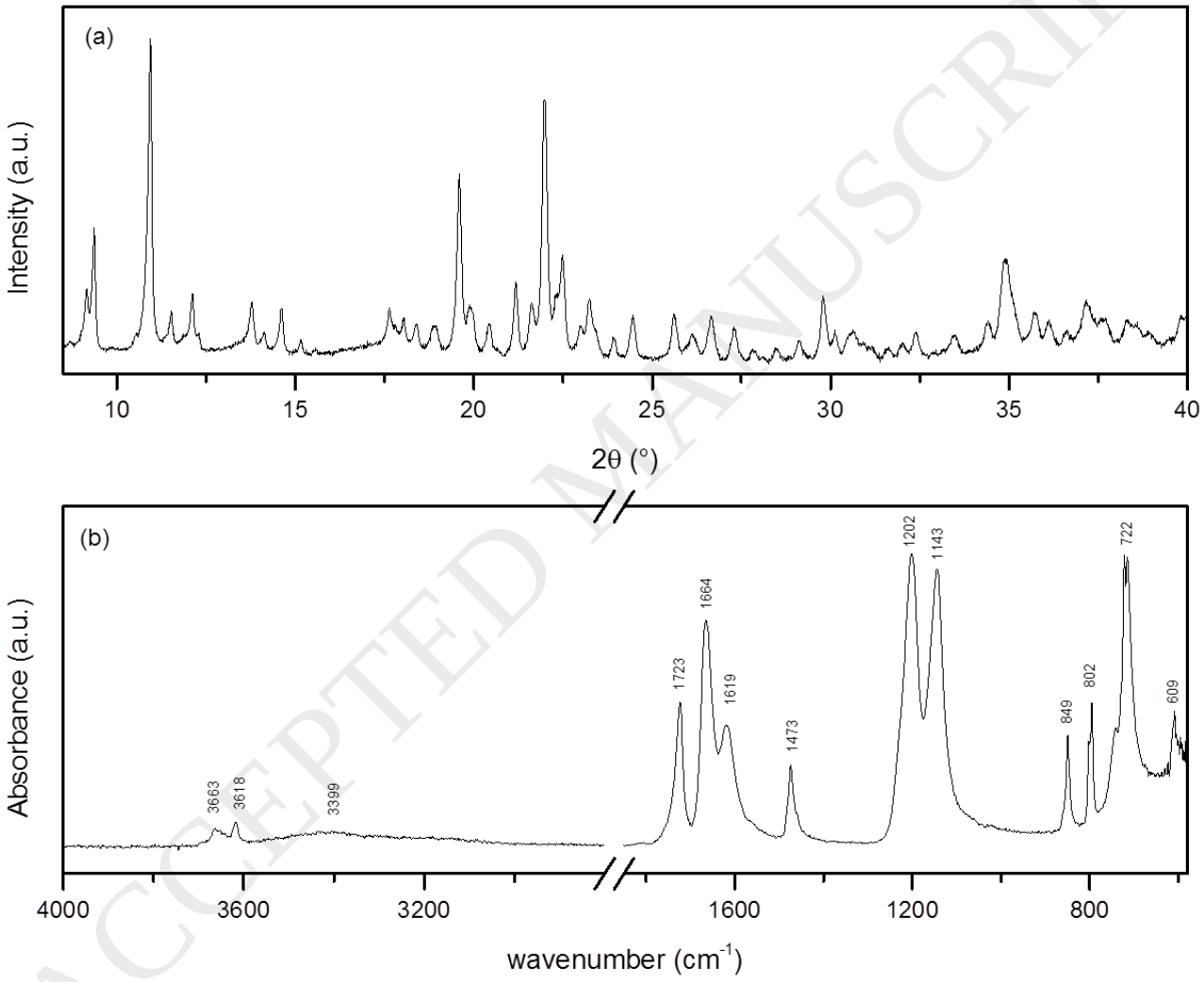

Figure 2.

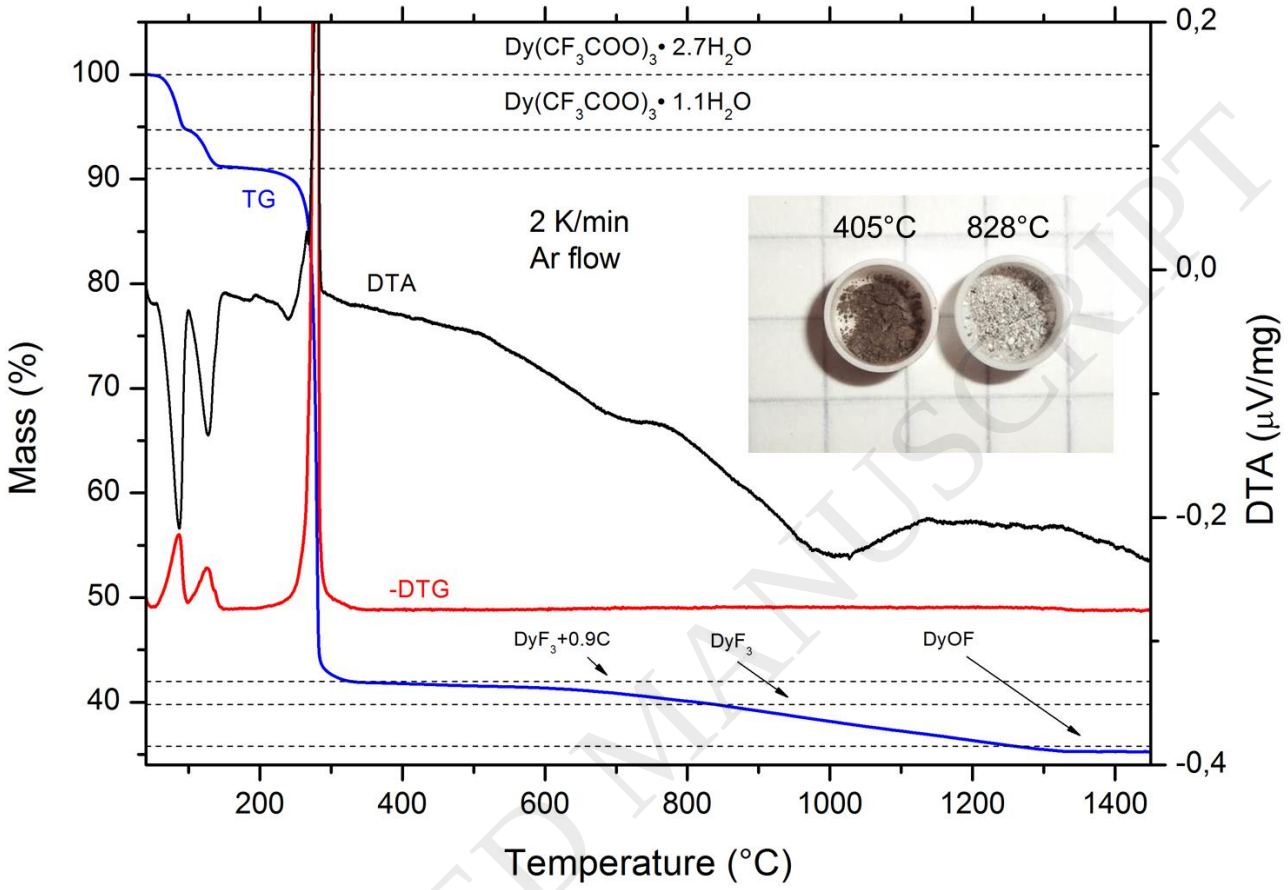

Figure 3.

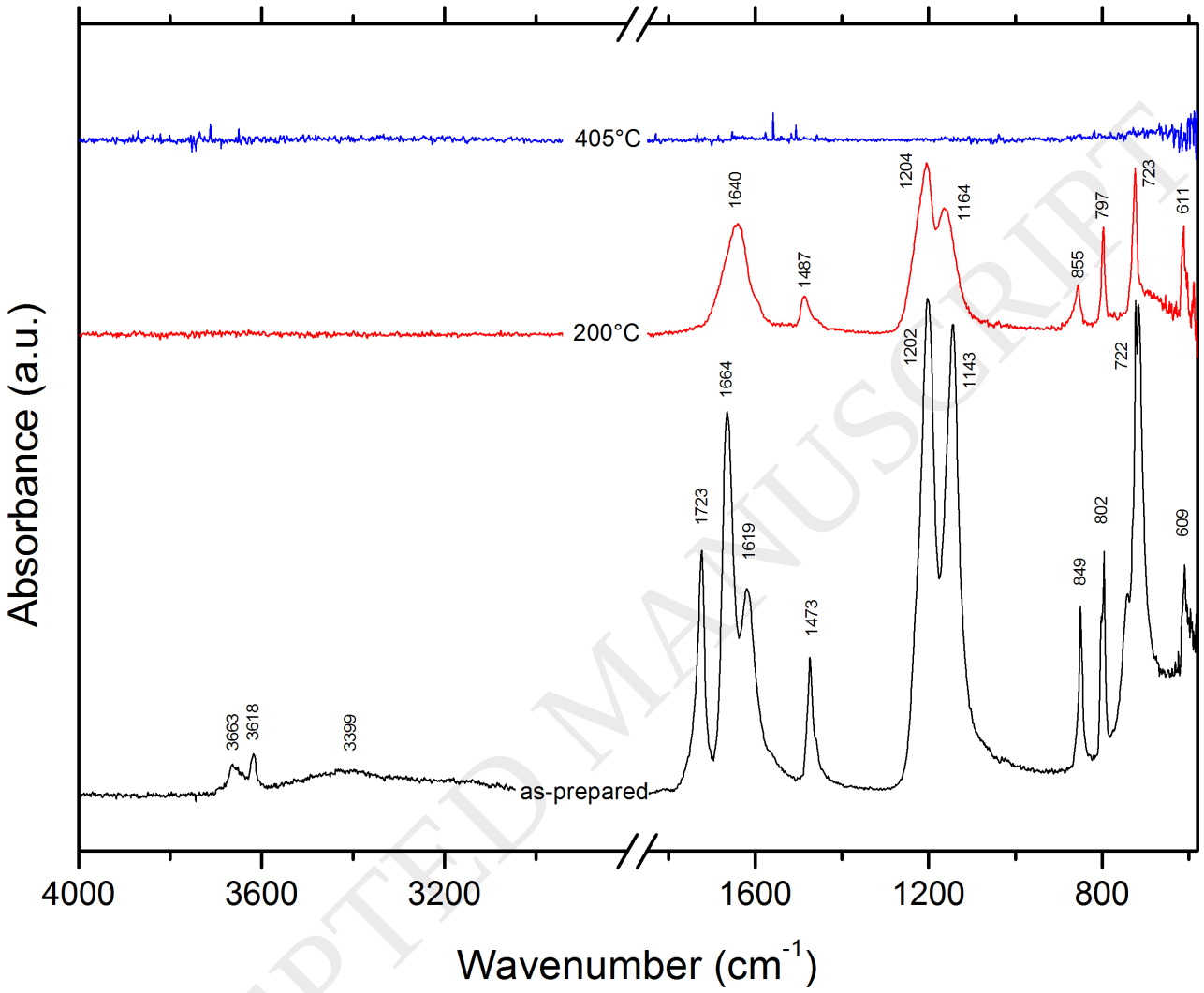

Figure 4.

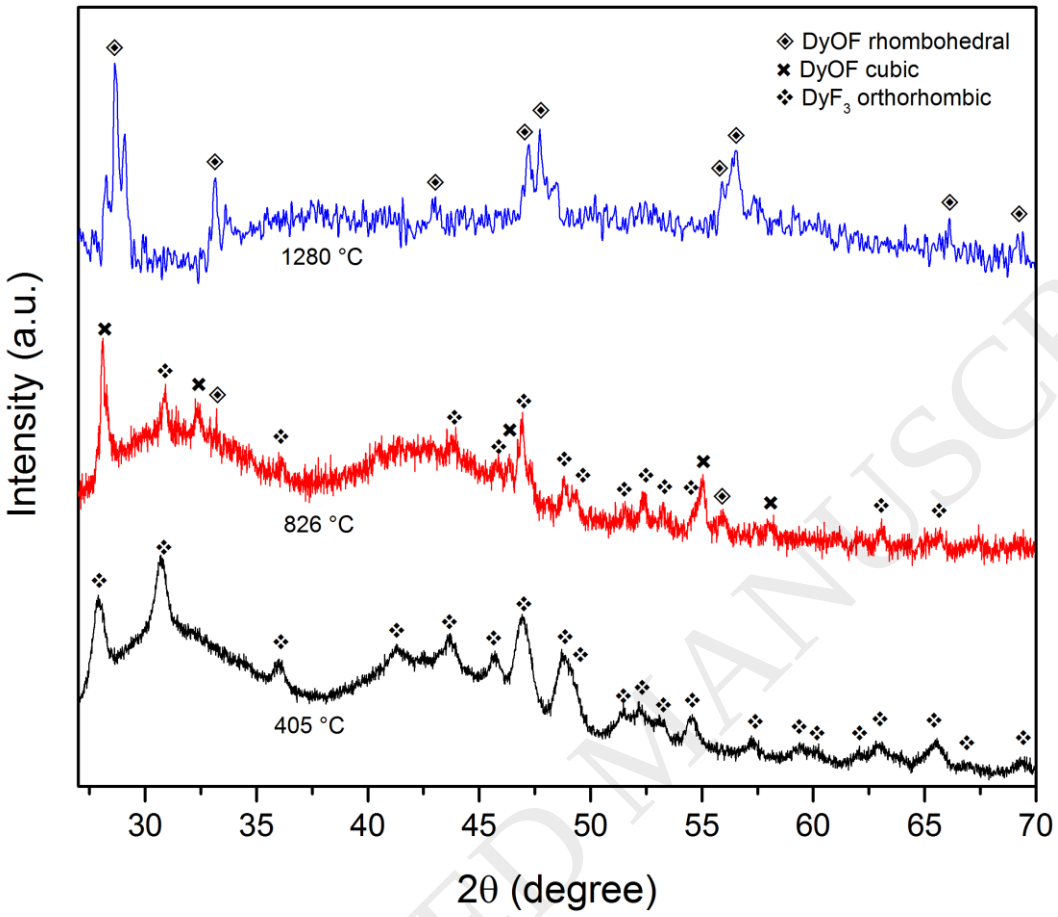

Figure 5.

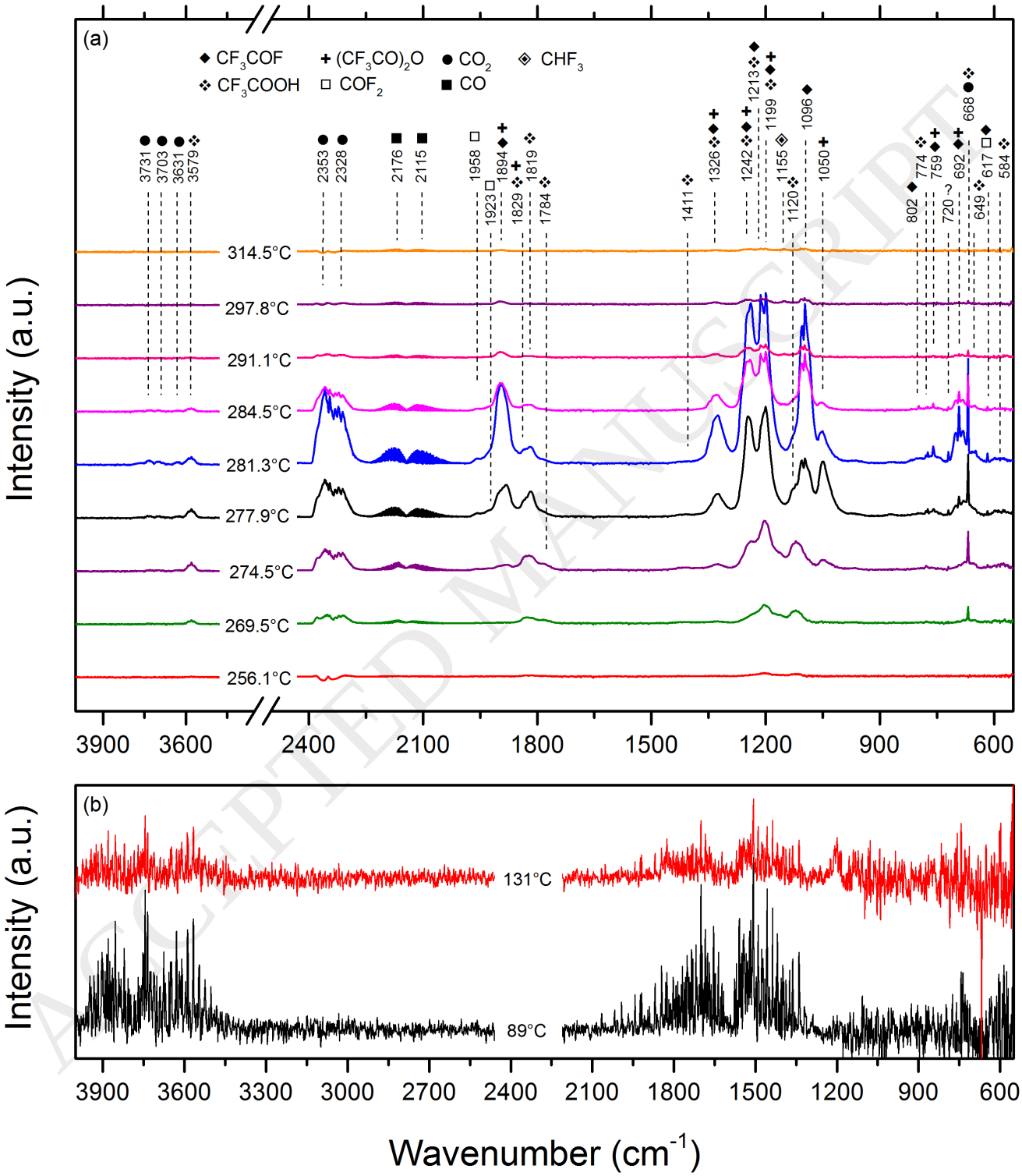

Figure 6.

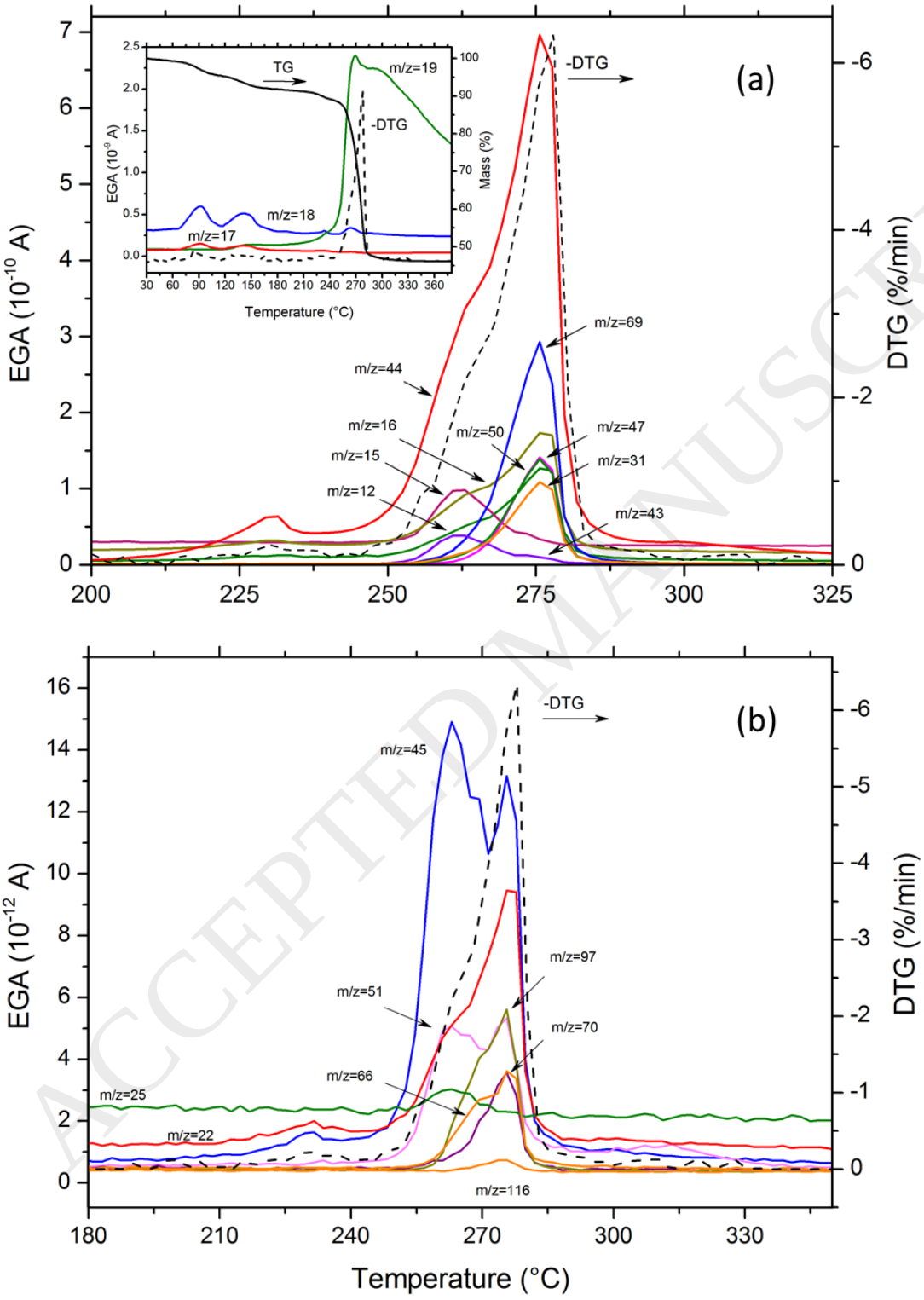

Table 1 – Observed absorption bands from FTIR data, acquired in the range 4000-550cm^{-1}. The assigned species and description is also presented.

Observed Peak wavenumber (cm^{-1})	**Species**	**Assignment**	**Reference**
3731	CO_2	C=O	[17, 24]
3703			
3631			
3579	CF_3COOH	O-H str.	[17, 26]
2353	CO_2	C=O asym. str.	[17, 24]
2328			
2176	CO	C≡O	[17, 24]
2115			
1958	CF_2O	C=O str.	[17, 24]
1923	CF_2O	C=O str.	[17, 24]
1894	$(CF_3CO)_2O$ CF_3COF	C=O str.	[17, 24, 27, 28]
1829	CF_3COOH $(CF_3CO)_2O$	C=O str.	[17, 26]
1819	CF_3COOH	C=O str.	[24]
1784	CF_3COOH	C=O str.	[25, 26]
1411	CF_3COOH	C-O str.	[17]
1326	$(CF_3CO)_2O$ CF_3COF CF_3COOH	C-F asym. str.	[17, 25, 27]

1242	$(CF_3CO)_2O$ CF_3COF CF_3COOH	C-F asym. str.	[25, 27, 28]
1213	CF_3COF CF_3COOH	FCF str. C-F str.	[24, 27]
1199	CF_3COOH CF_3COF $(CF_3CO)_2O$	C-F sym. str. C-C str.	[24, 27, 29]
1155	CHF_3	C-F str.	[17, 24]
1120	CF_3COOH	O-H ip. def.	[17]
1096	CF_3COF	C-F str.	[17, 24, 28]
1050	$(CF_3CO)_2O$	C-F str.	[17]
802	CF_3COF	C-C str.	[27, 28]
774	CF_3COOH	C-C ip. def.	[17, 26]
759	$(CF_3CO)_2O$ CF_3COF	C-F def.	[17, 27, 28]
720	unknown	unknown	
692	CF_3COF $(CF_3CO)_2O$	C-F def C=O def.	[17, 24, 27]
668	CF_3COOH CO_2	C=O def.	[17, 24]
649	CF_3COOH	C=O def.	[17]
617	COF_2, CF_3COF	C=O def.	[17, 24]
584	CF_3COOH	C-F ip. sym. def.	[17]

str.=stretching; def.=deformation; ip.=in-plane; sym.=symmetric; asym.=asymmetric.